JOURNAL OF Applied Polymer SCIENCE

Weld line improvement of short fiber reinforced thermoplastics with a movable flow obstacle

Marian Janko,[1] Bernhard Spiegl,[2] Andreas Kaufmann,[2] Thomas Lucyshyn,[1] Clemens Holzer[1]

[1]Department of Polymer Engineering and Science, Chair of Polymer Processing, Montanuniversitaet Leoben, 8700 Leoben, Austria

[2]HOERBIGER Ventilwerke GmbH & Co KG, 1110 Vienna, Austria

Correspondence to: C. Holzer (E-mail: clemens.holzer@unileoben.ac.at)

ABSTRACT: Short fiber reinforced (SFR) thermoplastics are ideal materials from which to manufacture complex technical parts in high volumes with low energy expenditure. The orientation of the fibers, and hence their reinforcing effect, depends strongly on the nature of the cavity and on the injection molding process. One disadvantage of SFR thermoplastics is a significant decrease in mechanical properties in the areas of the weld lines, due to **subopt**imal fiber orientation as the melt streams reunite at these points. Common mold-based and process-based optimization techniques alter the fiber orientation after the formation of the weld line. The mold-based approach presented here, on the other hand, operates at the time the weld line is formed: by redirecting the melt streams, it moves the weld line and improves the fiber orientation. A prototype mold is described, and samples produced from it with both standard and modified weld lines are **compared with** flawless specimens. The new technique yields a large rise in flexural strength and a smaller but significant improvement in tensile properties. © 2015 Wiley Periodicals, Inc. J. Appl. Polym. Sci. **2015**, *132*, 42025.

KEYWORDS: fibers; mechanical properties; molding; thermoplastics

Received 28 September 2014; accepted 26 January 2015

DOI: 10.1002/app.42025

INTRODUCTION

Injection molded short fiber reinforced (SFR) parts are used in various industrial fields because they meet the requirements of many technical applications. SFR molded products show several advantages for both manufacturers and users. The fiber reinforcement improves the mechanical properties of the thermoplastics used, giving them high stiffness and allowing them to bear high loads. This allows the production of technical parts with low effort, in a short time and with a high degree of automation. Complex SFR parts can be reproduced in large volumes and to close tolerances.

High part complexity, however, leads to one of the disadvantages of injection molded SFR parts: separation and rejoining of the melt during the molding process creates weld lines, which in turn compromise the mechanical properties. Especially in SFR parts, weld lines reduce the mechanical properties of the finished part to just 30 to 50% of those which characterize the bulk material.[1,2] The main reason for the weakness of the weld line region lies in the fiber orientation, which is very different from the orientation elsewhere. Specifically, the fibers in the bulk of the molding follow the flow direction, whereas in the weld line region they lie perpendicular to the flow direction. This unintended fiber orientation is the result of the "fountain flow" effect at the front of the melt streams.[3,4]

Poor fiber orientation leads to a low degree of reinforcement in the weld line regions, with consequently lower structural integrity and reliability. The effect of the weld line on the structural integrity is measured by a so-called weld line factor (WLF) A_{WL}. This is the ratio of a particular mechanical property measured in a part containing a weld line (P_{WL}) to the same property of a flawless part (P_{FL}) (Equation 1).

$$A_{WL} = \frac{P_{WL}}{P_{FL}} \tag{1}$$

There are several ways to improve SFR parts containing weld lines, ranging from simple optimization of process parameters to mold modifications and process rearrangement. For parameter optimization, the improvement potential depends strongly on the material and mold used. Some studies show no improvement at all, while others have succeeded in raising the strength of the finished part by up to 10%.[1,5]

A common mold-based approach is the use of proper venting, which is assumed to be important to avoid Diesel effects and entrapped air in the weld line.[1] An interesting technique is to use a multicavity mold in which an additional cavity is connected to the main cavity via a small gate. The additional cavity is filled right after the main cavity containing the weld line; by

creating a pressure difference, this forces the still-molten material to flow across the weld line and so reorients the fibers. This technique has been shown to give an increase of about 20% in the weld line strength of a 20 wt % glass fiber reinforced polycarbonate.[6]

The push-pull process (PPP) technique is more complicated, but uses the same idea of forcing melt through the weld line after it has formed. The necessary pressure difference is achieved with two injection units, which first inject simultaneously to fill the part. Once the weld line is formed, one injector "pushes" more melt into the mold while the other "pulls" surplus material out.[7] Originally invented to improve weld lines in liquid crystal polymers, PPP was also found to benefit SFR parts. Several studies show that PPP can improve the strength of SFR parts by 25 to 70%.[8–10]

All the mold- or process-based approaches, however, are difficult to implement on complex parts characterized either by multiple weld lines or by lack of room to add extra cavities. To get around these disadvantages, a technique which interferes directly with the process of weld line formation was developed in this work.

The new approach presented in this article can be implemented for one or more weld lines, involves no additional process modification, and needs no extra space in the parting plane, because it works behind the cavity. The basic idea is to interfere with the formation of the weld line as it emerges, and so to improve the resulting fiber orientation. In the region where the weld line is predicted to form, an obstacle is used to redirect the melt streams. This obstacle is designed to be pushed out of the cavity as the pressure in the weld line area approaches a certain filling pressure or the final holding pressure. A spring returns the obstacle to its original position after the part is ejected.

To test the concept a prototype mold was built which can produce two specimens at the same time: one containing a standard weld line and the other with a modified weld line. By changing the sprue system, the same mold can also yield flawless specimens for comparison. For this study polyether ether ketone (PEEK) reinforced with 30 wt % carbon fiber (CF) was used to produce samples for tensile and flexural testing.

Weld line modification increased the tensile strength by 22% and the tensile strain at strength by 28%, compared with specimens with standard weld lines. The results of the flexural tests, which were performed in two different configurations, were even more remarkable. The modification raises the flexural strength by 61 to 66%, depending on the test configuration, while the flexural strain at strength increased by 83 to 92%.

We also made flawless specimens and tested them to calculate the WLFs. Modification of the weld line increased the WLF from 0.44 to 0.55 for tensile strength and from 0.44 to 0.74 for flexural strength. For flexural strain at strength, using the new technique increased the WLF from 0.53 to 1.03.

This article presents a new mold-based technique for improving weld lines in SFR parts, together with the technical implementation in a specimen prototype mold and the results of monotonic flexural and tensile tests.

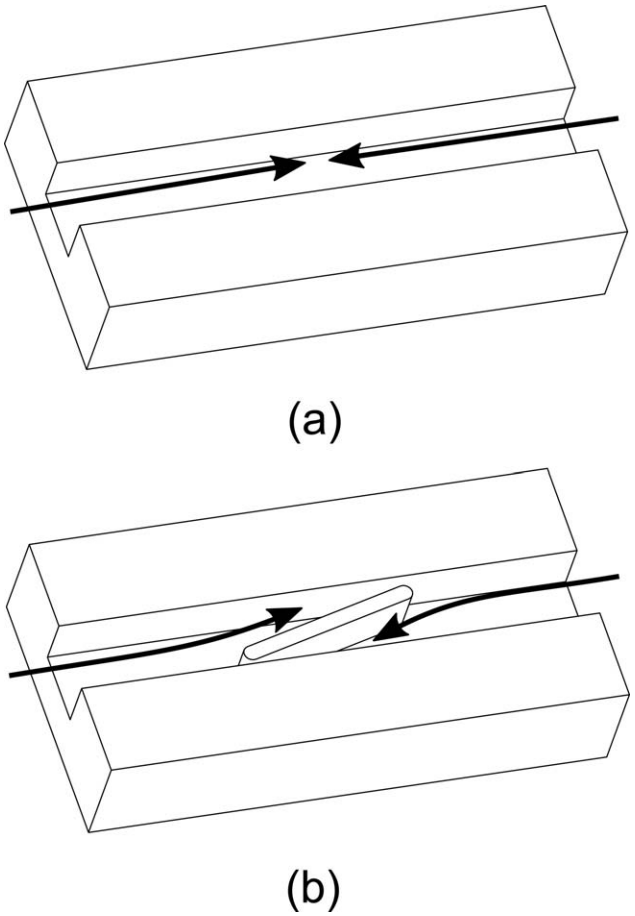

Figure 1. (a) In a standard mold channel, melt streams entering from left and right form a conventional cold weld line at the point where they meet (for clarity, the upper mold surface is not shown). (b) By disrupting the melt flows, a removable obstacle can change the nature of the junction between the two streams.

EXPERIMENTAL

Technology Background

The main weakness caused by the weld line comes from the orientation of fibers in this region. The natural orientation, at right angles to the flow direction, is not well adapted to withstanding applied loads, especially tensile loads in the flow direction. The idea of reorganizing the fibers in the weld line area is not new, and is used in both the multi-gate and PPP techniques. Here, the fiber orientation is altered after the weld line has formed, by introducing a pressure difference which creates flow through the weld line.

This article instead presents a technique involving active interference at the time of weld line formation. The idea is to use a flow obstacle placed in the cavity to redirect the melt streams in the weld line area. The change in flow direction alters the fiber orientation and so improves the mechanical properties. Figure 1(a) shows a standard flow channel: melt streams moving in from the left and right create a conventional cold weld line in the middle. Figure 1(b) shows how an obstacle inserted in the weld line region can redirect the flows, guiding the melt streams

to opposite sides of the channel and hence changing the way in which the weld line area fills.

To get a completely filled part an additional process step is necessary: removing the obstacle from the mold as soon as it has done its job of reorienting the melt streams. To withdraw the obstacle from the mold, it has to be ensured that the obstacle is free to move perpendicular to the parting plane. This can be done by a pneumatic or electric actuator, or more simply by using the pressure of the melt itself to push the obstacle out of the mold.

The latter technique can be achieved by ensuring that the obstacle does not fill the cavity completely, but instead has a small gap separating it from the opposite mold surface. Once the obstacle has redirected the melt streams, this gap fills with molten polymer, the pressure of which acts to push the obstacle out of the cavity. A spring behind the obstacle ensures that it re-enters the mold after the part has been ejected.

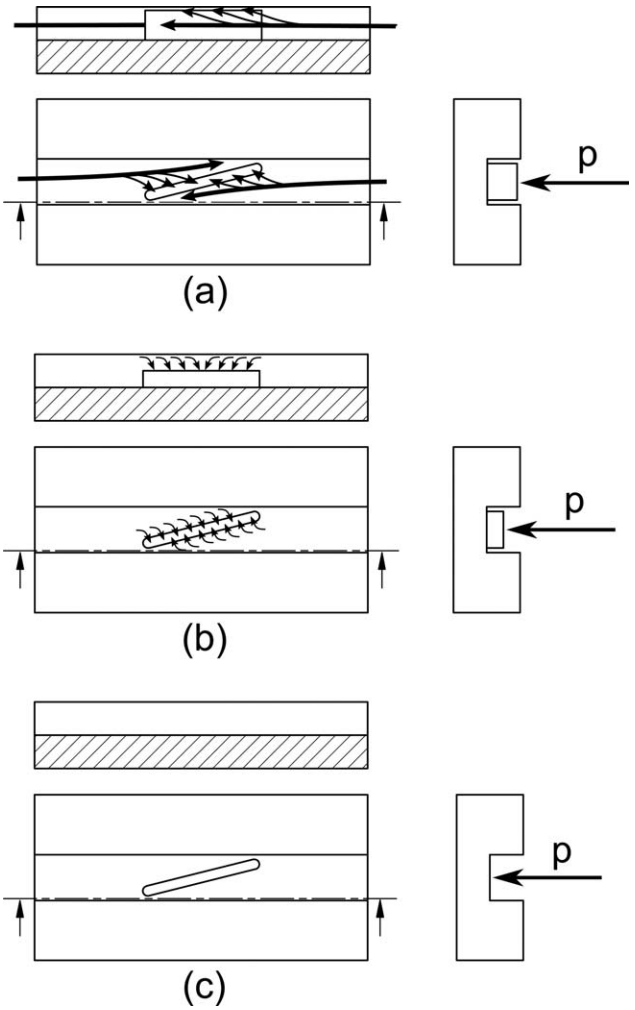

Figure 2. (a) As the obstacle diverts the melt flows entering the mold from left and right, material also begins to enter the narrow gap between the top surface of the obstacle and the opposite mold face. (b) Rising pressure on the top surface starts to push the obstacle out of the mold. (c) The obstacle in its fully withdrawn position. Once the part is ejected, a spring moves the obstacle back into the cavity in preparation for the next shot.

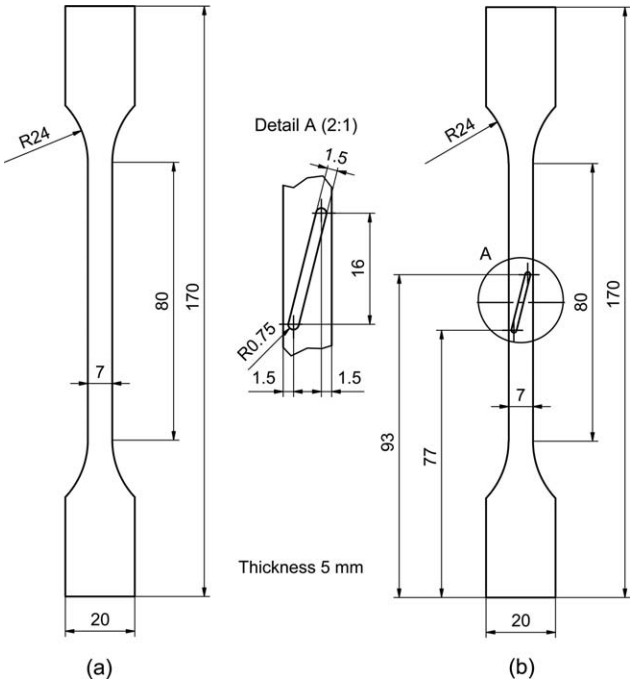

Figure 3. The test mold has two cavities: one (a) produces specimens with a standard weld, while the other (b) has a movable flow obstacle. Detail A shows the obstacle at 2:1 scale. All dimensions in millimeters.

Figure 2 shows the complete filling procedure in three steps. In Figure 2(a), the obstacle protrudes into the channel, leaving a narrow gap between its top edge and the opposite mold surface (which for clarity is not shown). Melt entering from the left and right (heavy arrows) is diverted to each side of the obstacle, and also begins to fill the gap (light arrows).

In Figure 2(b), the rising pressure created by the melt has begun to act on the top surface of the obstacle, pushing it out of the cavity. In Figure 2(c) the obstacle is fully ejected, allowing melt to fill the space it previously occupied. The ejection of the obstacle can take place in either the filling or the holding phase, depending on the process conditions.

Prototype Mold

To verify the concept a prototype mold was built. This is based on a standard weld line specimen mold with two cavities, one of which is fitted with a spring-loaded movable obstacle (Figure 3).

The cavities are similar to those described by specimen design 1A of the ISO 527-2 standard, modified to be closer to the geometry of the future target application. The specimen's cross-section is 7×5 mm^2, compared with 10×4 mm^2 for the original ISO specimen.

Each cavity is gated from both ends to produce a weld line in the middle. This allowed a comparison of the properties of two different specimens produced in a single shot: one with a weld line modified by the presence of the obstacle, the other with a standard weld line. Due to a simple sprue modification it is possible to produce single-gated ("flawless") specimens without weld lines.

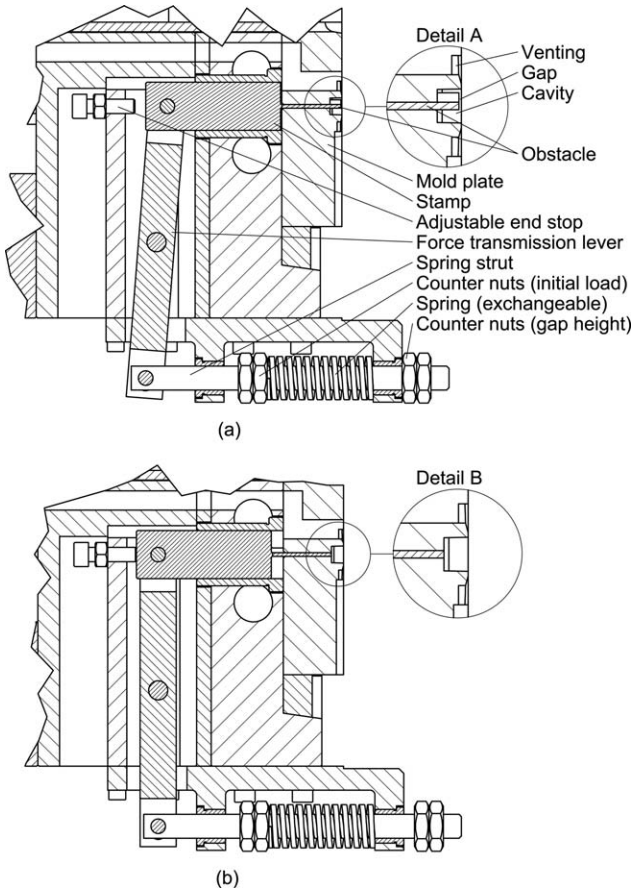

Figure 4. Detailed sectional views of the ES of the prototype mold: (a) the filling phase, and (b) after the obstacle has withdrawn from the cavity.

Figure 4 gives detailed sectional views of the ejection side (ES) of the mold, showing the position of the movable obstacle during the filling phase [Figure 4(a)] and in its withdrawn position [Figure 4(b)]. The obstacle is mounted on a stamp and guided by the mold plate. The stamp is connected to a transmission lever which is pivoted at its center and connected at its other end to an external spring mechanism which forces the obstacle into the mold. The use of interchangeable springs with an adjustable preload (via the left-hand pair of counter nuts) makes it easy to test the effect of different spring characteristics.

The counter nuts on the right are used to adjust the immersion depth of the obstacle and hence the initial width of the gap between the top of the obstacle and the opposite mold surface.

The position of the obstacle at the other end of its movement—when it has been pushed out of the mold—is controlled by a screw and nut behind the stamp. It may be important to withdraw the obstacle far enough to allow some of the melt to be squeezed out of the cavity through the obstacle slot, carrying with it any material that has solidified at the surface of the obstacle (see below).

Figure 4 also shows the cross-section of the generously designed venting system, which runs along the whole contour of the specimen. The venting system is designed to provide optimal mold venting and hence the best possible weld line quality.

The mold is heated by electric elements at both the ES and the nozzle side (NS), each controlled by a temperature sensor.

When the mold is opened, the spring acting on the obstacle creates an extra load on the specimen. This is countered by a pneumatic cylinder which acts on the transmission lever during the opening and ejection sequence. By implementing the obstacle mechanism into the NS, this problem does not occur and there is no need for a pneumatic cylinder.

Injection Molding

Injection molding experiments were carried out with a 30 wt % CF-reinforced PEEK on an ENGEL e-motion 940/280 injection molding machine. Three types of specimens were produced: standard weld line; modified weld line; and no weld line ("flawless").

Table I lists the basic injection molding parameters and specific mold settings, the latter having been discovered from preliminary tests. A series of preliminary tests revealed that the spring constant and initial load had little influence on the nature of the weld line, and needed only be set high enough to ensure the proper return of the obstacle to its initial position. For the main experiments, a spring with a rate of 2.8 N mm^{-1} was used with an initial spring load of 14 N. A gap width of 0.5 mm was found to be the smallest value at which the obstacle was ejected reliably.

It was also investigated how varying the position of the obstacle end stop influenced the weld line properties of the specimen. For this purpose two types of specimen were produced. In the first, the material in the region of the obstacle slot was flush with the main surface of the specimen (no protrusion). In the second type, the end stop was adjusted so that the material in the slot area protruded by around 0.7 mm; this excess was then ground off before testing. The preliminary tests showed no significant differences in tensile or flexural properties between specimens produced with and without protrusions. For ease of specimen preparation, therefore, in all subsequent shots the end stop was adjusted to produce specimens without protrusions.

Measurement Setup

The monotonic flexural and tensile properties of the specimens – no weld line, standard weld line and modified weld line,

Table I. Injection Molding and Mold Settings

Parameter	Value
Switch-over point	Volumetric at approximately 99%
Injection rate (cm^3 s^{-1})	25
Nozzle temperature (°C)	420
Mold temperature (°C)	210
Holding pressure (MPa)[a]	70
Cooling time (s)	30
Spring constant (N mm^{-1})	2.8
Initial spring load (N)	14
Gap height (mm)	0.5

[a] Applied for 10 s.

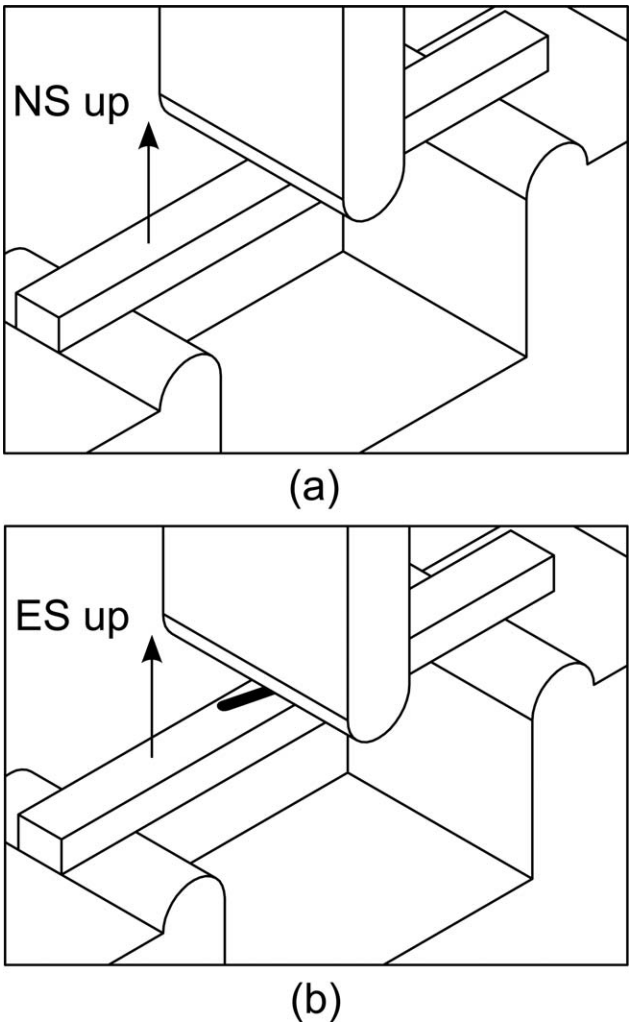

Figure 5. Flexural properties were tested in two configurations: (a) NS uppermost; (b) ES uppermost, showing the mark left by withdrawal of the obstacle.

respectively—were tested. The following subsections present the test procedures in more detail.

Flexural Measurement Setup. The flexural properties were measured with a three-point bending fixture mounted in a Zwick Roell Z010 testing machine. The specimens were prepared by cutting an 80 mm length from the middle section.

Because the obstacle is inserted and ejected from one side of the mold, the fiber orientation varies across the thickness of the specimen, so flexural tests must be performed from both sides (Figure 5). Figure 5(a) shows the specimen placed with its NS upwards; Figure 5(b) shows the ES upwards, and the surface mark left after ejection of the obstacle. To ensure that the stress field in the weld line is the same in every test, the loading pin was placed directly above the weld line or the middle of the obstacle mark. Five specimens were tested at each setting. Table II lists the parameters used.

The force and the crosshead displacement, which represents the deflection, are used to calculate flexural stress and strain based on the equations given in the ISO 178 standard, assuming linear elastic behavior. As specified by the standard, the flexural modulus of the specimens is taken to be the secant modulus calculated at flexural strains of 0.05% and 0.25%.

Table II. Parameters for Flexural Testing

Parameter	Value
Fixture	Three-point bending
Control type	Position control
Strain measurement	Crosshead displacement
Radius fixed support (mm)	5
Radius loading pin (mm)	5
Fixed support distance (mm)	60
Force transducer (kN)	10
Initial load (N)	10
Testing rate (mm min^{-1})	20
Temperature (°C)	23
Rel. humidity (%)	50

Tensile Measurement Setup. The monotonic tensile properties of the specimens were also investigated. The tests were again performed on the Zwick Roell Z010, with a wedge-screw grip fixture and an extensometer placed in the middle of the specimens with a gage length of 60 mm. Five specimens of each type were tested. Specimens were prepared by removing the sprue system. Table III shows the parameters used.

The recorded force and length difference measured with the extensometer were used to calculate tensile stress and strain according to ISO 527. Calculations based on the engineering strain (i.e. based on the original dimensions of the specimen) are acceptable because the high fiber loading results in small deformations and maximum strains. As with the flexural measurements, the tensile modulus is taken to be the secant modulus.

RESULTS AND DISCUSSION

Short Shots

To investigate the filling behavior of the cavities, short shots were made and photographed (Figure 6). As the "a" series of

Table III. Parameters for Tensile Testing

Parameter	Value
Fixture	Wedge-screw grips
Control type	Position control
Strain measurement	Contact-type extensometer
Clamping length (mm)	125
Gage length (mm)	60
Force transducer (kN)	10
Initial load (N)	10
Testing rate (mm min^{-1})	1.25
Temperature (°C)	23
Rel. humidity (%)	50

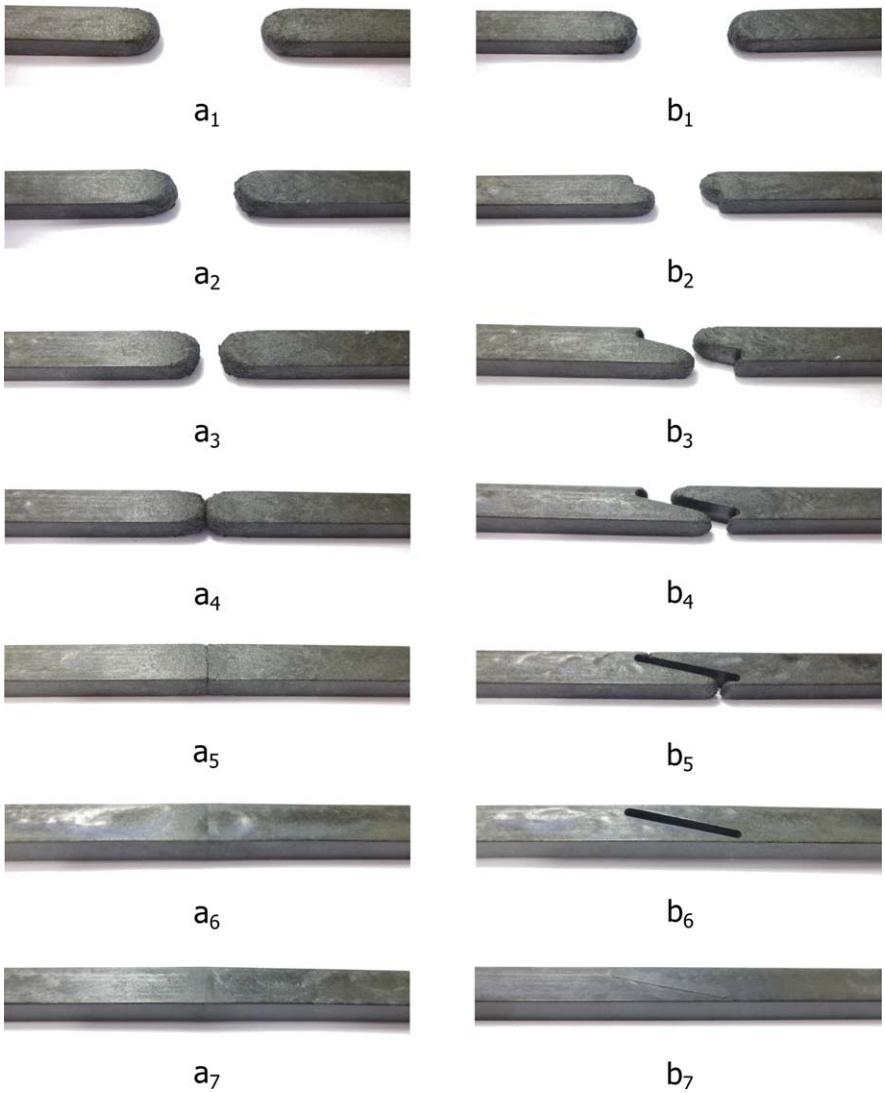

Figure 6. Consecutive short shots of standard weld line specimens (a_1–a_7) and modified weld line specimens (b_1–b_7). [Color figure can be viewed in the online issue, which is available at wileyonlinelibrary.com.]

images shows, in the standard specimen cavity the two melt streams meet along a line at right angles to the long axis of the cavity. With the obstacle in place ("b" series), most of each melt stream is deflected along the face of the obstacle, while a small proportion passes around the nearer end of the obstacle. As each of these two smaller streams meets the main stream on the other side of the obstacle it creates a small "side weld line." The two side weld lines significantly affect the mechanical properties of the specimen (see below).

Once the melt fills the entire cavity except for the space occupied by the obstacle [Figure 6(b6)], melt pressure in the gap between the top of the obstacle and the mold surface forces the obstacle out of the cavity. This step is hard to visualize via short shots, however, so the next image [Figure 6(b7)] shows the final specimen after holding and cooling. During the holding and cooling phases, fluid pressure prevents the spring from pushing the obstacle back into the mold until the specimen has hardened sufficiently.

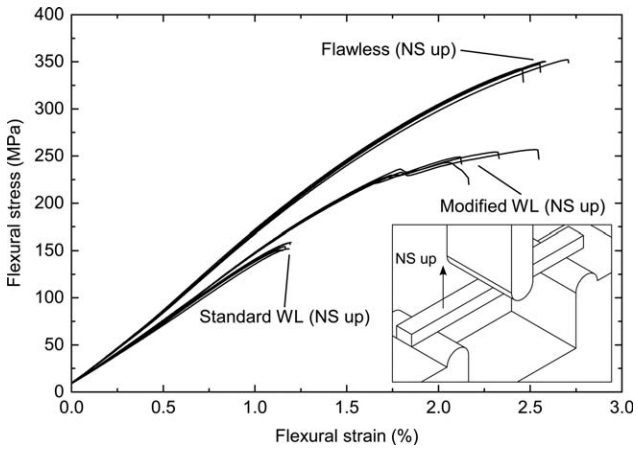

Figure 7. Flexural stress–strain curves of flawless, standard, and modified weld line (WL) specimens tested in the "NS up" configuration.

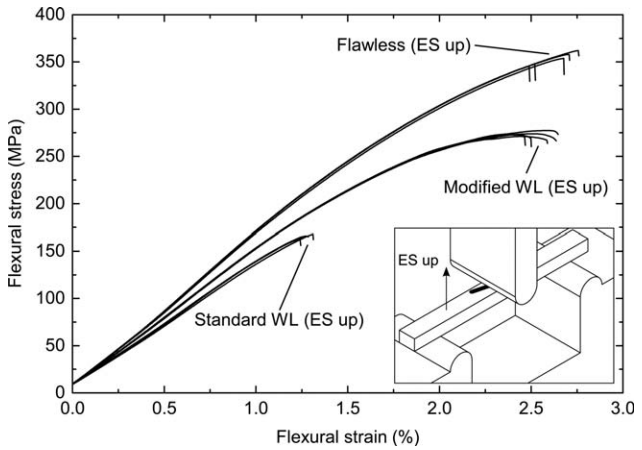

Figure 8. Flexural stress-strain curves of flawless, standard, and modified weld line (WL) specimens tested in the "ES up" configuration.

Flexural Tests

Figure 7 shows the measured flexural stress–strain curves for the flawless, standard, and modified weld line specimens tested in the "NS up" configuration. The flawless specimens show the highest values, with an average flexural strength of 372 MPa and an average strain at strength of 2.4%, while the modified specimens reached an average strength of 250 MPa and an average strain at strength of 2.2%. The standard specimens show the lowest values, with an average strength of 155 MPa and an average strain at strength of 1.2%. The modification of the weld line therefore gave an improvement of 61% in strength and 83% in strain. The WLFs for the standard specimens are 0.42 for flexural strength and 0.49 for strain at strength. The modified specimens reached WLFs of 0.67 for strength and 0.93 for strain at strength.

All the stress-strain curves for the modified specimens show a kink at around 1.8% flexural strain. This is assumed to be due to an initial crack in the side weld line, which can be seen in the fracture surfaces (discussed further below). This initial crack does not lead to immediate failure of the whole specimen, which endures a further deformation of around 0.4%. This fracture behavior is assumed to be responsible for the greater variability in flexural strain at strength in the modified weld line specimens (standard deviation 0.18%, compared with 0.02% for the standard weld line specimens).

Figure 8 shows the flexural stress-strain curves of the "ES up" configuration. The flawless specimens tested in this configuration (average flexural strength 372 MPa, average strain at strength 2.4%) show no difference from those for the "NS up" configuration. The modified weld line specimens reached an average flexural strength of 274 MPa and an average flexural strain at strength of 2.5%, without the kinks seen in Figure 7. The standard weld line specimens showed an average flexural strength of 165 MPa and an average flexural strain at strength of 1.3%. The modification of the weld line therefore gave an improvement of 66% in strength and 92% in strain.

The calculated WLFs of the modified specimens are 0.74 for flexural strength and 1.03 for strain at strength. These figures are higher than for the "NS up" configuration (0.67 for strength and 0.93 for strain at strength). The difference is assumed to be connected to the fiber orientation in the region representing the original gap between the obstacle and the NS. We can assume that in this test the flexural strength is determined by the tensile strength near the bottom face of the specimen, where the tensile stress is highest. The higher strength values obtained in the "ES up" configuration seem to show that the fiber orientation is better near the NS, or less good near the ES.

The NS region contains the former gap between the top of the obstacle and the wall. The filling of this gap produces just one long weld line, slanted at almost the same angle as the obstacle itself, so it appears that the fiber orientation in this region is good. On the other hand, the small side weld lines which form at the side surfaces of the obstacle occur on the ES, and it seems that these are responsible for the relative weakness of the specimens in the "NS up" configuration.

The calculated WLFs for the standard weld line specimens (0.44 for flexural strength and 0.53 for strain at strength) are higher than those for the "NS up" configuration (0.42 for strength and 0.49 for strain at strength). This behavior is discussed below.

Even for the standard weld line specimens, the two flexural testing configurations show a small but significant difference in strength (155 MPa for "NS up," 162 MPa for "ES up"). This difference is not seen in the flawless specimens, and is probably due to asymmetric mold venting. The specimens show a rough weld line surface on the ES and a smooth surface on the NS. The rough side seems to bear lower tensile stresses, so the "ES up" configuration is stronger. The roughness in the weld line is assumed to be connected to a slight "v-notch," or simply bad bonding, where the melt streams meet on the ES. The effect seems to be linked with the fact that the mold is vented on the NS but not on the ES: better venting produces a smoother weld line.

In the modified weld line specimens, the slot for the obstacle acts as an additional vent on the ES. This surface of the modified weld line specimens is smooth, similar to the NS of the standard weld line specimens.

To sum up the flexural behavior of the different specimens, the crucial points are listed below:

- The standard weld line specimens show slightly better flexural performance in the "ES up" configuration compared with the "NS up" configuration; as explained above, this is probably due to the difference in venting;
- The modified weld line specimens show considerably better flexural performance, in both configurations, than the standard weld line specimens;
- For the modified weld line specimens, flexural performance is better in the "ES up" configuration;
- The flawless specimens show higher flexural strength than the modified weld line specimens, regardless of which side is uppermost;
- Due to their high degree of fiber alignment, the flawless specimens show lower flexural strain at strength compared with the modified weld line specimens in the stronger ("ES up") configuration.

Table IV. WLFs for Flexural Strength and Flexural Strain at Strength

	WLF for flexural strength	WLF for flexural strain
Standard WL (NS up)	0.42	0.49
Standard WL (ES up)	0.44	0.53
Modified WL (NS up)	0.67	0.93
Modified WL (ES up)	0.74	1.03

Table IV lists the corresponding WLFs, calculated using the flawless specimen values for bulk behavior. The excellent potential for improvement by using a movable obstacle is clear. In the stronger "ES up" test configuration, modifying the weld line raises the WLF for strength from 0.44 to 0.74, and for strain at strength from 0.53 to 1.03.

Figure 9 shows the average secant flexural modulus for the three types of specimen and the two configurations. The flawless specimens show the highest average modulus: 18 GPa. For the modified weld line specimens the modulus is about 5 GPa lower, with a small but significant difference between the test configurations (13.7 GPa for "ES up," 13.1 GPa for "NS up"). The value for the standard weld line specimens is slightly lower (about 12.6 GPa), with no significant difference between the two configurations.

The improvement in flexural modulus for the modified weld line specimens is assumed to be rooted in the way that the low-modulus weld line region is slanted, rather than perpendicular to the long axis as in the standard specimens. For the modified weld line specimens, the difference in modulus between the two configurations is connected to the differences in fiber orientation between NS and ES, due in turn to the process of filling and obstacle ejection.

Figure 10 shows photographs of the fracture surfaces for the different specimen types and test configurations. Though only one broken specimen of each type is shown, all the other specimens tested looked exactly the same. The fracture surface of a flawless specimen [Figure 10(a)] is rather rugged, and looks as if it has consumed a lot of energy in being torn apart. Everywhere in the specimen the fibers are oriented on the long axis

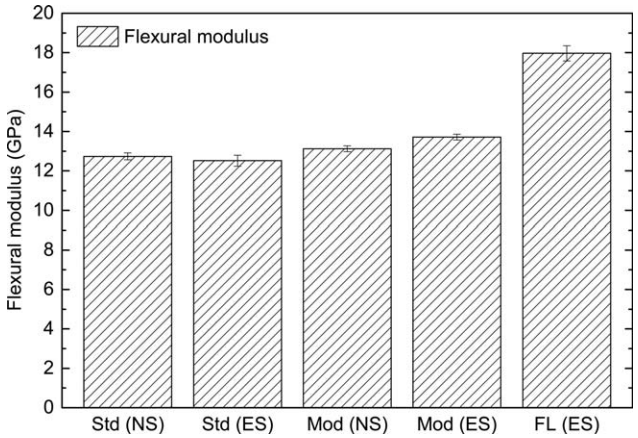

Figure 9. Average values and standard deviations of the flexural modulus for flawless (FL), standard (Std), and modified (Mod) weld line specimens, tested in both the "NS up" and "ES up" configurations.

of the specimen, creating the reinforcing which allows the specimen to withstand the high loads measured. All the flawless specimens broke exactly under the loading pin, where the highest stresses occur.

Figure 10(b) is a standard weld line specimen, showing a smooth fracture surface with no rough regions. Each of the standard weld line specimens broke exactly along the weld line, which was placed directly under the loading pin. As with the flawless specimens, the fracture surfaces look similar for the "NS up" and "ES up" configurations. The smooth surface reflects the fact that most of the fibers in the weld line region are perpendicular to the flow direction. With only few fibers to resist the principal stress, the maximum load the specimen can withstand is lower than in the case of the flawless specimens.

The modified weld line specimens tested in the "ES up" [Figure 10(c)] and "NS up" [Figure 10(d)] configurations show different fracture surfaces and crack paths. Much of the fracture surface is rugged, but there is a small strip of smooth surface on the left-hand side. This smooth strip is one of the two side weld lines, whose formation is shown in Figure 6(b5). These side weld lines occur where the main melt stream deflected by the obstacle meets the opposite stream which has flowed round the end of the obstacle. In the region of the side weld lines, the

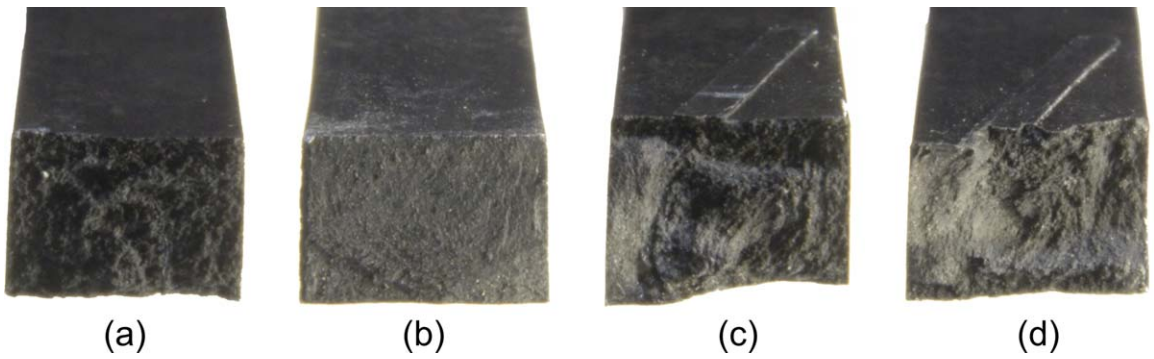

Figure 10. Fracture surfaces after flexural failure for flawless (a), standard weld line (b), modified weld line "ES up" (c), and modified weld line "NS up" (d) specimens. [Color figure can be viewed in the online issue, which is available at wileyonlinelibrary.com.]

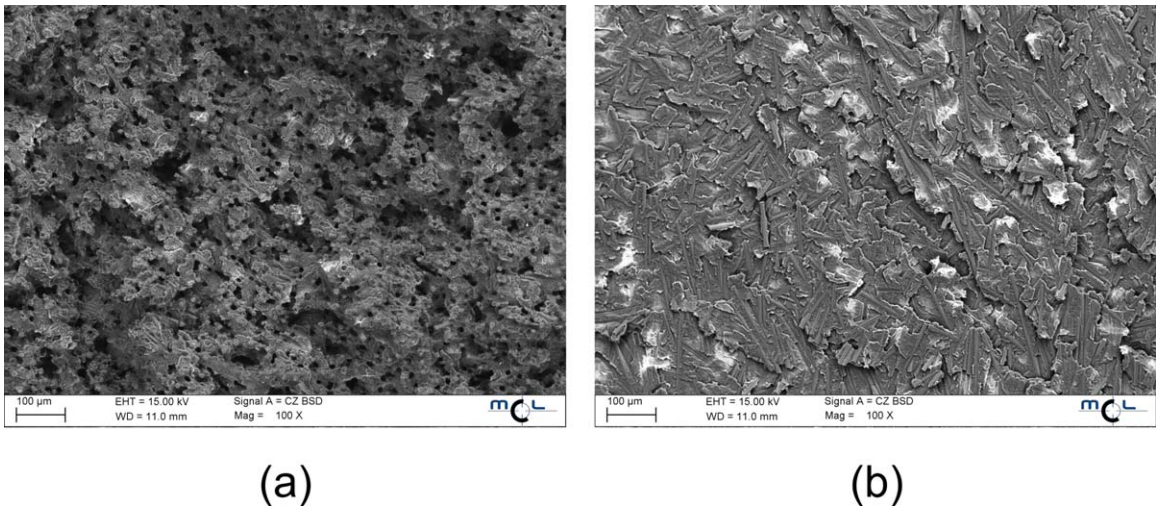

Figure 11. SEM micrographs taken at the middle of the fracture surface of the flawless (a) and standard weld line (b) specimens. [Color figure can be viewed in the online issue, which is available at wileyonlinelibrary.com.]

fibers are oriented similarly to those around a standard weld line, and the material is comparatively weak.

It can be assumed that where side weld lines are present, a crack initiates there before running through the stronger, more highly oriented, region created by the presence of the obstacle, and shown as the rugged region on the fracture surface. In the "ES up" configuration [Figure 10(c)] the crack begins at the lower left side, whereas in the "NS up" configuration [Figure 10(d)] it begins at the upper left side; in each case this in the tensile region.

It is also assumed that the third possible flexural test configuration—loading the side surface of the specimen—would show little or no improvement compared with a standard weld line specimen. In this case the maximum tensile stress would fall on the side weld line, which would be expected to fail at stress values very close to those measured for the standard weld line specimens.

For a closer inspection of the former fiber orientation at the fracture surfaces, micrographs were taken by means of a scanning electron microscope (SEM). Figure 11 shows micrographs taken at the middle of the fracture surface of the flawless [Figure 11(a)] and standard weld line [Figure 11(b)] specimens. At the flawless specimen, the magnified fracture surface shows holes (small circular black spots), some fibers protruding and like the macroscopic image a rather rugged overall surface. The small circular holes are assumed to be the remains of pulled out fibers. In contrast to that, the standard weld line specimen shows fibers which are orientated in the direction of the fracture surface, and an overall smooth surface appearance.

Figure 12 shows the fracture surfaces of the modified weld line specimens tested in the "ES up" configuration. The micrographs of the specimens tested in the "NS up" configuration were similar to them. The micrograph in Figure 12(a) shows the fracture surface in the rugged middle of the specimens, while the

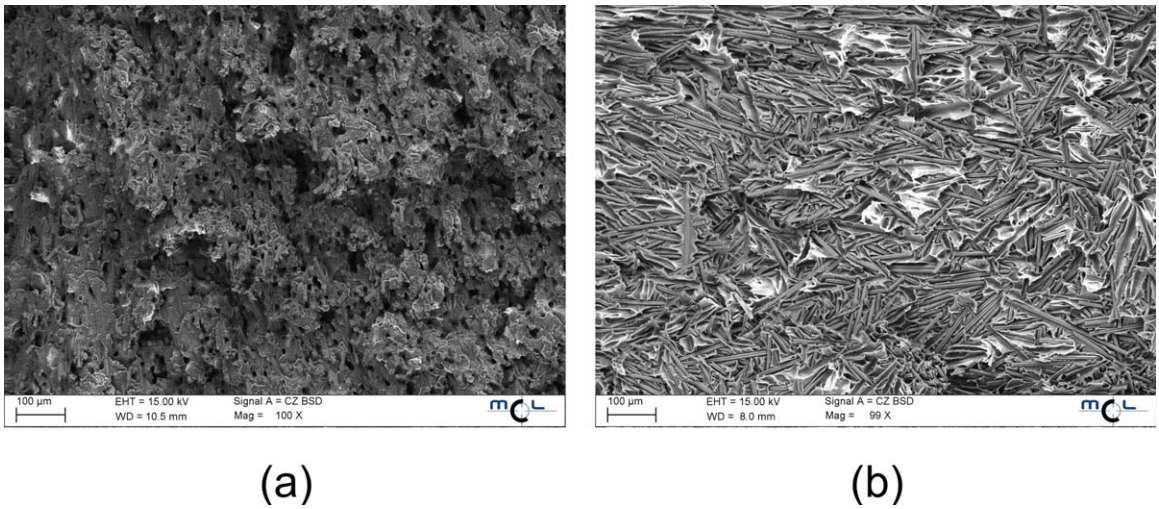

Figure 12. SEM micrographs of the modified weld line "ES up" fracture surface from the rugged middle (a) and the side weld line (b) region. [Color figure can be viewed in the online issue, which is available at wileyonlinelibrary.com.]

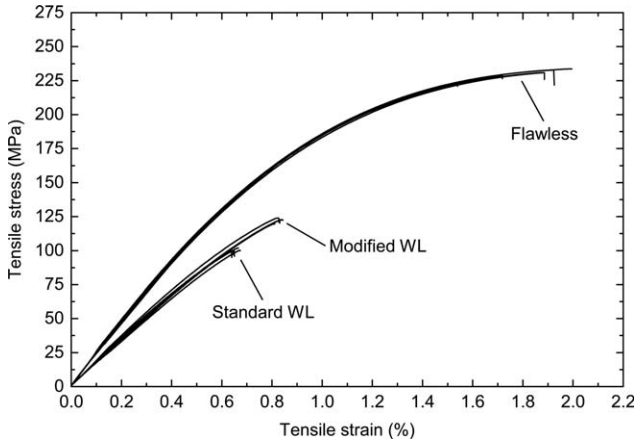

Figure 13. Tensile stress–strain curves for the flawless, modified and standard weld line (WL) specimens.

micrograph in Figure 12(b) was taken at the side weld line region. The middle regions are highly oriented similar to the flawless specimen (Figure 11). The fibers in the side weld line region seem to be oriented similar to the standard weld line fracture surface. The matrix of the standard weld line fracture surface seems to be very smooth and flaked off at some areas, whereas it seems to be torn apart at the side weld lines of the modified specimens. Maybe this is related to different joining temperatures or pressures, or result of the melt movement during the obstacle ejection.

Tensile Tests

The monotonic tensile properties of the flawless, standard and modified weld line specimens were also tested. The tensile performance is not crucial for the planned application, but may be of interest in other cases.

Figure 13 shows the measured tensile stress–strain curves. The flawless specimens perform by far the best, reaching an average tensile strength of 230 MPa and a tensile strain at strength of 1.8%. Up to around 0.3% strain the behavior is approximately linear, followed by softening until breakage. The standard weld line specimens reach an average tensile strength of 100 MPa and a strain at strength of 0.65%. The effect of weld line modification is lower in the pure tensile stress tests. Weld line modification produces a modest improvement compared with the standard weld line, with an average strength of 122 MPa (22% greater) and a strain at strength of 0.83% (28% greater). The WLFs for tensile strength are about 0.44 for the standard and 0.53 for the modified specimens.

Table V shows the calculated weld line factors. These confirm the low performance of all the weld line specimens compared with the flawless specimens. Modifying the weld line increases the tensile performance significantly, but even so the resulting specimens achieve only about the half the performance of the flawless specimens. The big improvement seen in the flexural tests is not repeated in the pure tensile tests. This is because the modification transforms the perpendicular weld line into a slanted one, which spreads the stress better under flexural loads. The modification still allows small weld lines to form at the sides of the specimen, however, and in tension these initiate cracks which lead to failure of the whole structure.

Table V. WLFs for Tensile Strength and Tensile Strain at Strength

	WLF for tensile strength	WLF for tensile strain
Standard WL	0.44	0.36
Modified WL	0.53	0.45

For the standard weld line specimens, the tensile strength WLF is in the same range as for the flexural tests. For strain at strength, on the other hand, the tensile WLF (0.36) is much lower than the flexural value (approximately 0.5). This behavior is assumed to relate to the fact that the flexural test exposes only the outer layer to the maximum flexural strain and stress. The outer layer is to some extent supported by the interior region, where the stress and strain are lower.

Weld line modification is not as effective for tensile as for flexural loading. The tensile WLFs are 0.53 for strength and 0.45 for strain, compared with flexural WLFs of 0.74 for strength and 1.03 for strain (in the "ES up" configuration). The weak spot of the modified specimens seems to be the side weld line. This small weld line is about 1 mm broad and runs along almost the whole height of the specimen, except the former gap on the NS of the specimen (Figure 15, below). It is assumed that the crack initiates in this region and weakens the whole specimen, which then fails immediately. Each of the modified weld line specimens tested shows the same fracture surface, including the failed side weld line.

Figure 14 shows the calculated average secant tensile moduli. The average modulus of the flawless specimens was about 23 GPa and shows the enormous influence of the fiber orientation. The average moduli of the two types of weld line specimens are both about 17 GPa, with no significant difference between them.

Figure 15 shows examples of the tensile fracture surfaces. Those for the flawless [Figure 15(a)] and standard weld line [Figure 15(b)] specimens look similar to those from the flexural tests

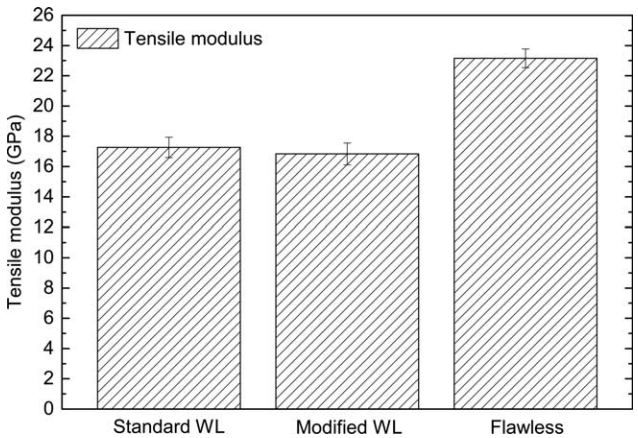

Figure 14. Average values and standard deviations of the tensile modulus for flawless, standard, and modified weld line (WL) specimens.

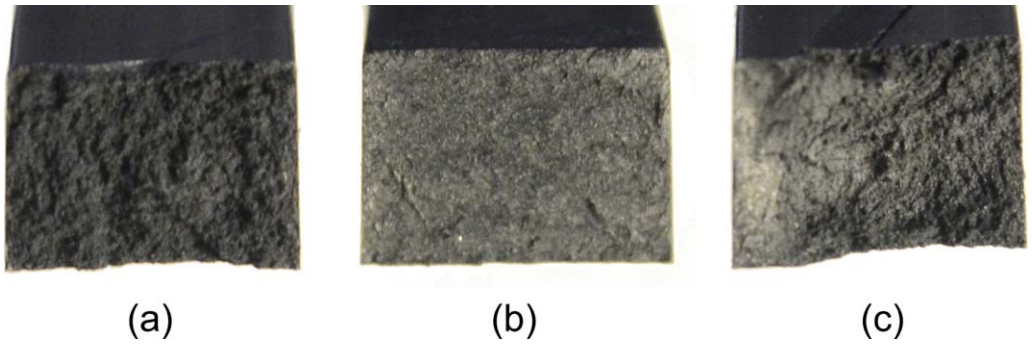

Figure 15. Tension fracture surfaces of (a) flawless, (b) standard, and (c) modified weld line specimens. [Color figure can be viewed in the online issue, which is available at wileyonlinelibrary.com.]

(Figure 10). The fracture surface of the flawless specimen [Figure 15(a)] shows a rather rugged surface, with fibers oriented in the test direction over the whole cross-section. With a high degree of reinforcement and no particular weak points, these specimens broke at different locations along their length. The smooth fracture surface of the standard weld line specimen [Figure 15(b)] is the exact opposite. Most of the fibers in the weld line region are aligned perpendicular to the test direction, producing a weak line along which every specimen broke.

The fracture surface of the modified weld line specimen [Figure 15(c)] looks like a mixture of the two others. A small strip on the left side looks like the fracture surface of the standard weld line, while the rest is rugged, like the fracture surface of the flawless specimen. The mark of the obstacle top is visible at the top of the photograph, which gives information about the longitudinal position of the fracture. All these specimens broke at one end of the obstacle, at the exact location of the side weld line. Since the weld line is weak, we assume that the crack initiates in this region. The remainder of the cross-section then sees a sudden jump in stress, and fails immediately.

The taken SEM micrographs of the fracture surfaces after tensile failure show similar structures to the ones of the flexural tests.

CONCLUSIONS

This article presents a novel mold-based weld line optimization technology. It outlines the basic concept of using a movable obstacle to redirect the melt, after which the rising melt pressure ejects the obstacle automatically. Three types of specimens were produced: one with a standard weld line, one with a weld line modified by use of the obstacle, and one with no weld line.

Monotonic tensile and flexural tests were used to quantify the weld line improvement. The asymmetric geometry, required to eject the obstacle, results in a fiber orientation which varies through the thickness of the specimen; to measure how this affected the mechanical properties, the flexural tests were therefore performed from both sides of the specimen.

The flexural results for the specimens with modified weld lines showed significant differences according to which side was uppermost in the test rig, but overall there was a big improvement in both flexural strength (up to 66%) and flexural strain at strength (up to 92%) compared with specimens with standard weld lines. Changing the standard perpendicular weld line to one running at an angle, with a corresponding change in fiber orientation in the weld line region, yields this huge improvement in the flexural properties. The reason for the dependence on the tested specimen side is found in the presence of so called "side weld lines," which are created during the filling phase. Although smaller and therefore less problematic than standard full-width weld lines, under high tensile stresses side weld lines do provide points for fractures to start. As a result, the fracture surfaces of the modified weld line specimens reveal a mixed appearance, with smooth surfaces representing the side weld lines and larger, rough areas like those found in flawless specimens.

Taking this logic further, the limitations of the modified weld line technique become apparent under pure tensile testing. Here the improvement compared with standard weld lines is about 20% for tensile strength. It is assumed that the small side weld lines are responsible for this relatively modest improvement: the fibers in these regions are perpendicular to the applied tensile stress, giving the weld line low strength and allowing cracks to start in this region. Once a crack has formed, the load-bearing area decreases instantly, increasing the stress in the remaining cross-section and leading to complete failure.

Modifying the position, angle and shape of the obstacle to avoid or minimize the side weld lines, and implementing the technology in complex cavities, are the next research targets.

ACKNOWLEDGEMENT

The research work was carried out within a project funded by HOERBIGER at the Montanuniversitaet Leoben at the Chair of Polymer Processing. The author thanks HOERBIGER for providing excellent support and especially Dr. Bernhard Spiegl, who had the original idea for this technology.

REFERENCES

1. Cloud, P. J.; McDowell, F.; Gerakaris, S. *Plast. Technol.* **1976**, *22*, 48.
2. Fisa, B.; Rahmani, M. *Polym. Eng. Sci.* **1991**, *31*, 1330.
3. Rose, W. *Nature* **1961**, *191*, 242.

4. Templeton, P. A. J. *Reinf. Plast. Compos.* **1990**, *9*, 210.
5. Seldén, R. *Polym. Eng. Sci.* **1997**, *37*, 205.
6. Hamada, H.; Maekawa, Z.; Horino, T.; Lee, K.; Tomari, K. *Int. Polym. Proc.* **1988**, *2*, 131.
7. Gutjahr, L.; Becker, H. *Kunststoffe* **1989**, *79*, 1108.
8. Ludwig, H. -C.; Fischer, G.; Becker, H. *Compos. Sci. Technol.* **1995**, *53*, 235.
9. Patcharaphun, S. J. *Reinf. Plast. Compos.* **2005**, *25*, 421.
10. Tomari, K.; Takashima, H.; Hamada, H. *Adv. Polym. Technol.* **1995**, *14*, 25.